Asymptotic analysis of boundary effects on concrete fracture

K. Duan & X.Z. Hu
School of Mechanical Engineering, University of Western Australia, Crawley, Australia

F.H. Wittmann
Qingdao Technological University, Qingdao, China and Aedificat Institute Freiburg, Germany

ABSTRACT: The recently-developed boundary effect concept and associated asymptotic model are used to analyse the various size-dependent fracture behaviours of concrete specimens. It is shown that the dependence of concrete fracture on specimen size, crack and/or ligament length is due to the same mechanism, i.e. the interactions between the crack tip fracture process zone and specimen boundaries. By introducing an equivalent crack a_e, all these dimension dependent fracture behaviours become equivalent to a large plate with a small edge crack, and therefore, follow the same relationship of the "net" nominal strength σ_n versus a_e. As a result, the size dependent fracture can be predicted using the data measured on different types of specimens. To demonstrate the flexibility and effectiveness of the asymptotic boundary effect model, three previous experimental results available in the literature are analysed, and excellent agreements are achieved. Furthermore, the implications behind the successful predictions are discussed.

1 INTRODUCTION

"Size effect" in concrete fracture has been a hotly-debated topic for nearly half a century because of its important implications to the applications of fracture mechanics to concrete structures. Since Kaplan reported the dependence of fracture toughness on beam depth in 1961 (Kaplan 1961), extensive experimental observations on the size dependence of fracture behaviours have been documented. The main size dependent behaviours include (1) the fracture energy of concrete specimens increases with increasing ligament, (2) the fracture strength of non-geometrically similar specimens increases with decreasing ligament and/or crack length, and (3) the strength of geometrically similar specimens decreases with increasing specimen size (Higgins & Bailey 1976, Nallathambi et al. 1985, Hashida & Takahashi 1985, Shinohara et al. 1991, Karihaloo et al 2003). This size dependence of fracture diminishes and the fracture parameters become material constants when the corresponding dimension is very "large". Therefore, the size-independent fracture parameters required for the structural integrity analysis of concrete structures can only directly be measured on "huge" fracture mechanics specimens, which are often impractical for many laboratories.

Alternatively, these size-independent fracture properties can be extrapolated from the size-dependent fracture data measured on the laboratory-sized specimens. This requires an appropriate fracture mechanics model relating the specimen size and geometry to the fracture behaviours. Over the past three decades, a number of fracture mechanics models have been developed including the ficticious crack model (Hillerborg et al 1976) and two-parameter model (Jenq & Shah 1985) for the ligament-dependent fracture energy, and a few "size effect" models (Bažant 1984, Carpinteri et al 1995, Karihaloo 1999), which consider the relationship between the strength and size of geometrically similar specimens. These models have been used to analyse the fracture behaviours of concrete specimens and to predict the size-independent fracture parameters.

The authors have recently developed the boundary effect concept and two fracture mechanics models to characterize the size dependent fracture properties (Hu & Duan 2002, Duan & Hu 2002, 2004, Duan et al. 2002, 2003a,b, 2004, 2006). The boundary effect concept explains the size dependence of the fracture energy and strength as a result due to the interactions between the specimen boundaries and crack tip fracture process zone (FPZ). When the crack tip is close to a specimen boundary, the specimen boundary will limit the development of the FPZ, and therefore, lead to a reduced fracture energy. Meanwhile, a fracture mechanics specimen with either a short crack or ligament will fracture in a more "ductile" manner. The "ductile" failure is controlled by the maximum tensile stress. When the maximum tensile stress reaches the material tensile strength f_t, the specimen fails. On other hand, when

the FPZ is far away from specimen boundaries, the specimen strength is determined by the linear elastic fracture mechanics (LEFM) criterion.

This paper aims to explain the asymptotic boundary effect model. For this purpose, the influence of the specimen boundaries on concrete fracture is firstly analysed by considering the role of the boundaries in dominating the failure mode. Then, three sets of fracture testing data available in the literature are analysed using the asymptotic boundary effect model. It will be shown that the predictions from the asymptotic model agree very well with those measured data, and the implications behind this agreement are discussed.

2 BOUNDARY EFFECT CONCEPT AND ASYMPTOTIC MODEL FOR FRACTURE STRENGTH OF CONCRETE

The boundary effect concept is explained in Figure 1 where a finite-sized plate with a single edge crack is subjected to a remote applied load. Depending on the closeness of the crack tip FPZ to either boundary, the strength of the plate can be determined by either the material tensile strength f_t or fracture toughness K_{IC}. When the crack tip is close to the front boundary (short crack) as shown in Figure 1a, the crack will be shielded before specimen failure, and therefore, the plate strength is determined by the maximum tensile stress condition (f_t). On the other hand, when the FPZ is close to the back boundary (short ligament, Fig. 1c), the ligament will "yield" prior to the final fracture, the failure of the plate is again controlled by f_t. Only when the crack tip locates in the middle of the plate where it is far away from both boundaries, is the plate strength decided by the LEFM criterion (Fig. 1b).

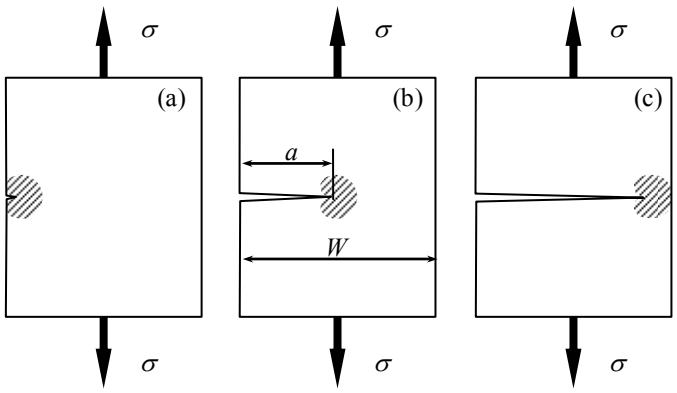

Figure 1. The dependence of failure mode on the crack-tip-to-boundary distance: (a) a short crack is likely shielded before specimen failure; (b) crack tip is far away from both boundaries, and the LEFM dominates failure; and (c) a short ligament "yields" before final failure

Recently, an asymptotic boundary effect model has been developed to describe the afore-discussed relationship between the distance of the crack tip FPZ to specimen boundaries and the strength behaviours of fracture mechanics specimens (Duan & Hu 2002, 2004, Duan et al. 2006). This asymptotic solution for finite-sized specimens is based on the equivalent relationship between finite-sized specimens and a large plate with a small edge crack, and includes the σ_f-condition as asymptote for short crack or ligament and K_{IC}-criterion for a specimen with the crack tip away from boundaries.

The large plate case can be obtained when the specimen width $W >>$ crack size a in Figure 1, i.e. the ratio of the crack length a over the plate width W is equal to zero ($\alpha = a/W = 0$), and as a result, only specimen front boundary will influence specimen strength. The asymptotic solution for the simple large plate case was proposed by Hu and Wittmann (Hu & Wittmann 2000), and is given by:

$$\sigma_n = \frac{f_t}{\sqrt{1 + a/a^*_\infty}} \tag{1}$$

in which, the reference crack a^*_∞ represents the crack length where the two asymptotic limits intersects, and is given by:

$$a^*_\infty = \frac{1}{1.12^2 \pi}\left(\frac{K_{IC}}{f_t}\right)^2 \tag{2}$$

From Equation 1, the maximum tensile stress theory is obtained when $a << a^*_\infty$, and the LEFM criterion is recovered when $a >> a^*_\infty$.

$$\sigma_n = f_t \qquad a << a^*_\infty \tag{3a}$$

$$\sigma_n = \frac{f_t}{\sqrt{a/a^*_\infty}} = \frac{K_{IC}}{1.12\sqrt{\pi a}} \qquad a >> a^*_\infty \tag{3b}$$

The asymptotic solution, Equation 1 can be extended to a finite-sized specimen by establishing the equivalent relationship between the finite-sized specimen and the large plate. This can be achieved by comparing the f_t and K_{IC} criteria for the finite-sized specimen to those for the large plate as given in Equation 3. For this purpose, two nominal strengths, σ_n and σ_N can be defined for a fracture mechanics specimen. As shown in Figure 2, the nominal strength σ_N is based on the gross cross-section, and describes the failure stress of the specimen without considering the presence of the crack while the σ_n represents the net cross-section based failure stress without considering the stress concentration and singularity associated with the crack. These two nominal strengths are related each other by:

$$\sigma_N = \mathrm{A}(\alpha)\sigma_n \tag{4}$$

where A(α) reflects the influence of specimen geometry through its dependence on the ratio of the crack length a over characteristic size W ($\alpha = a/W$), and can be estimated through a mechanics analysis. For example, the A(α) functions for the fracture mechanics geometries given in Figure 2 are derived as:

$$\mathrm{A}(\alpha) = \frac{(1-\alpha)^2}{1+2\alpha} \qquad \text{SENT} \qquad (5a)$$

$$\mathrm{A}(\alpha) = \frac{(1-\alpha)^2}{2(2+\alpha)} \qquad \text{CT} \qquad (5b)$$

$$\mathrm{A}(\alpha) = (1-\alpha)^2 \qquad \text{3PB} \qquad (5c)$$

Obviously, A(α) is always lower than unity because σ_n is always higher than σ_N. Using the nominal strengths defined in Figure 2, the maximum tensile stress theory for a finite-sized specimen remains same as Equation 3a, and the LEFM criterion is given by:

$$K_{IC} = Y(\alpha)\cdot\sigma_N\sqrt{\pi a} \qquad (6)$$

in which $Y(\alpha)$ is a geometrical factor that can be found in many fracture mechanics texts and handbooks (e.g. Tada et al. 2000). For the convenience of further analysis, the $Y(\alpha)$ expressions for the three geometries shown in Figure 2 are listed as follow:

$$Y(\alpha) = \sqrt{\frac{2}{\pi\alpha}\cdot\tan\left(\frac{\pi\alpha}{2}\right)}\cdot\frac{0.752+2.02\alpha+0.37\cdot(1-\sin(\pi\alpha/2))^3}{\cos(\pi\alpha/2)} \qquad \text{SENT} \qquad (7a)$$

$$Y(\alpha) = \frac{(2+\alpha)(0.886+4.64\alpha-13.32\alpha^2+14.72\alpha^3-5.6\alpha^4)}{\sqrt{\pi\alpha}(1-\alpha)^{3/2}} \qquad \text{CT} \qquad (7b)$$

$$Y(\alpha) = \frac{1.99-\alpha\cdot(1-\alpha)\cdot(2.15-3.93\cdot\alpha+2.7\cdot\alpha^2)}{\sqrt{\pi}\cdot(1+2\cdot\alpha)\cdot(1-\alpha)^{3/2}} \qquad \text{3PB} \qquad (7c)$$

Combining Equations 2, 4 and 6, the LEFM criterion is re-written as:

$$\sigma_n = \frac{\sigma_N}{\mathrm{A}(\alpha)} = \frac{K_{IC}}{\mathrm{A}(\alpha)Y(\alpha)\sqrt{\pi a}} = \frac{f_t}{\sqrt{a_e/a_\infty^*}} \qquad (8)$$

where

$$a_e = a\cdot\left[\frac{\mathrm{A}(\alpha)\cdot Y(\alpha)}{1.12}\right]^2 \qquad (9)$$

It can be seen clearly that Equation 8 can be transformed to Equation 3b if a_e is replaced by a. Therefore, the strength behaviour of a finite-sized specimen is in fact, an equivalence of a large plate with a small edge crack a_e, and can be characterized by an asymptotic equation similar to Equation 1.

$$\sigma_n = \frac{f_t}{\sqrt{1+a_e/a_\infty^*}} \qquad (10)$$

It is interesting to note here that for both the SENT and 3PB specimens where $Y(\alpha)$ factors given in Equation 7 apply to $\alpha \rightarrow 0$, $W >> a$ will lead to $Y = 1.12$, A(α) = 1 and $\sigma_n = \sigma_N$. From Equation 9, one can get that $a_e = a$, and as a result, the asymptotic solution given in Equation 1 for the large plate case is recovered from Equation 10.

Re-arranging Equation 10, the linear form of the asymptotic model, which is often preferred for the analysis of experimental data, is given as:

$$\frac{1}{\sigma_n^2} = \frac{1}{f_t^2} + \frac{1}{f_t^2}\cdot\frac{a_e}{a_\infty^*} \qquad (11)$$

3 STRENGTH BEHAVIOURS OF FRACTURE MECHANICS SPECIMENS DUE TO BOUNDARY EFFECTS

3.1 *Crack and ligament dependence of strength resulting from boundary effects*

Boundary influence on the strength behaviours of fracture mechanics specimens is reflected in the a_e variations with the crack and ligament lengths through its equivalent relationship to the crack length in the large plate. The relationship between the equivalent crack a_e and α-ratio for SENT specimens is shown in Figure 3a where it can be seen that a_e reduces dramatically when α approaches either 0 or 1, and peaks when α is around 0.2. The maximum a_e is dependent on specimen size because of the limitation of the specimen size on the crack tip location. Corresponding to a_e variation as shown in Figure 3a, the nominal strength σ_n will approach to the maximum strength σ_f at both the front (α = 0) and back boundaries (α = 1), and is equal to the minimum strength at the maximum a_e (Fig. 3b). Depending on the specimen size W, the minimum strength can be determined by σ_f and/or K_{IC} criteria.

Shown in Figure 3c are the plots of the nominal strength σ_n versus the equivalent crack length a_e of both finite-sized SENT specimens and the large plate in the system of Ln σ_n versus Ln a_e. It is clearly shown that the strength of the large plate is bounded by the two asymptotic criteria, σ_f and K_{IC} criteria. For a short crack, i.e. the crack tip is close to the only boundary, σ_n is controlled by the maximum tensile stress theory, and for a long crack, i.e. the crack tip is far away from the front boundary, the LEFM criterion dominates the fracture of the large plate. In the quasi-brittle region, the gradual transi-

tion curve joins the asymptotes, σ_f theory and the K_{IC} criterion.

The σ_n-a_e curves of the finite-sized SENT specimens follow the strength curve of the large plate to the maximum a_e, and then turn back towards the asymptote of σ_f. The levels of the maximum a_e and therefore, the minimum σ_n are dependent on the specimen characteristic size W because of its physical limitation.

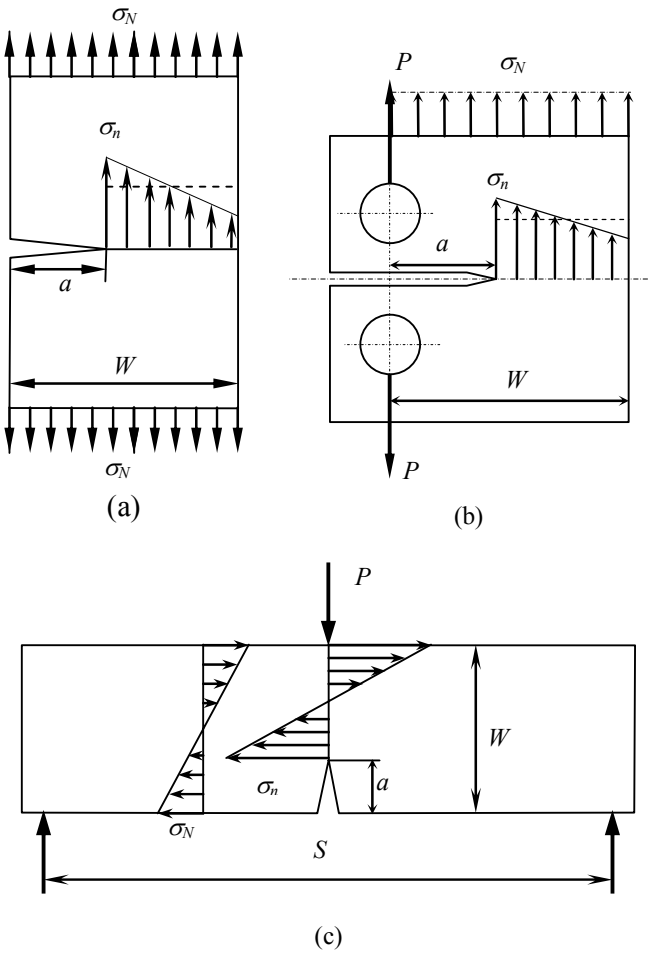

Figure 2. Specimen geometries for fracture mechanics study: (a) single-edge-notched tensile (SENT) specimen; (b) compact tension (CT) specimen; and (c) 3-point-bend (3PB) specimen.

3.2 *A special case of boundary effect: Size effect in the strength of geometrically similar specimens*

An interesting case in the size effect study is the geometrically similar specimens when the α-ratio is kept constant. As a result, the failure mode and strength of these specimens vary only with the specimen size. The previous "size effect" models including the size effect law (SEL) consider primarily the strength behaviours of geometrically similar specimens, and to verify these "size effect" models, many experimental studies on the geometrically similar specimens have been reported (Bažant 1984, Carpinteri et al 1995, Karihaloo 1999, Karihaloo et al. 2003). The size effect law is widely adopted for size effect study and relates the nominal strength σ_N of geometrically specimens to size W by:

$$\sigma_N = \frac{A_1 \cdot f_t}{\sqrt{1 + W/W_1}} \tag{12}$$

where the material tensile strength f_t is measured in a separate test, and A_1 and W_1 are two empirical constants, which are dependent on the α-ratio. For a given α value, separate experiments have to be performed to determine the two constants. As a result, it is not possible to predict the strength of a set of geometrically similar specimens without testing the specimens with same α-ratio.

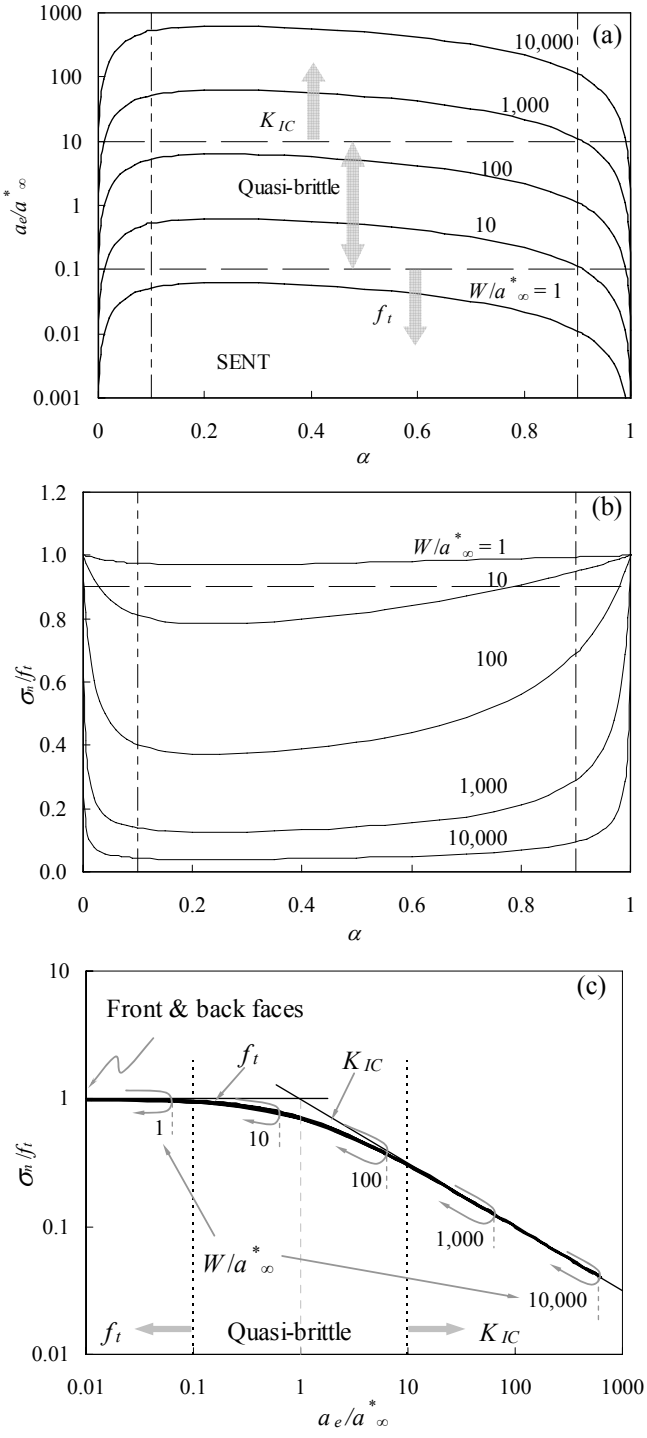

Figure 3. The influence of specimen boundary on failure mode and fracture strength: (a) the equivalent crack a_e and (b) nominal strength σ_n variations with α–ratio; (c) the relationship between σ_n and a_e or a.

On other hand, the strength behaviour of geometrically similar specimens can also be analysed using the asymptotic model given in Equation 10. For this purpose, substituting α = constant into Equations 9 and 10, the asymptotic equation is reduced to:

$$\sigma_n = \frac{f_t}{\sqrt{1+W/W^*}} \tag{13a}$$

or

$$\sigma_N = \mathrm{A}(\alpha)\cdot\sigma_n = \frac{\mathrm{A}(\alpha)\cdot f_t}{\sqrt{1+W/W^*}} \tag{13b}$$

where W^* is a constant for a given loading configuration and specimen geometry, and is referred to as the transition specimen size (Duan & Hu 2004).

$$W^* = W\cdot\frac{a^*_\infty}{a_e} = \frac{a^*_\infty}{\alpha\cdot\left[\dfrac{\mathrm{A}(\alpha)\cdot Y(\alpha)}{1.12}\right]^2} \tag{14}$$

It can be seen here that Equation 13b has a format similar to Equation 12. However, the explicit expressions are given in Equation 13 instead of the two empirical constants used in Equation 12. This is important because the two parameters can be calculated if specimen geometry and any two properties of f_t, a^*_∞ and K_{IC} are known, and using the two known parameters and specimen geometries, the nominal strength σ_n of specimens with different α-ratios can be predicted without further experiments. Furthermore, it is not necessary that a separate experiment is performed to measure f_t because it can be calculated from fracture mechanics test.

4 ANALYSIS AND DISCUSSION OF THE LITERATURE DATA USING ASYMPTOTIC BOUNDARY EFFECT MODEL

4.1 *Strengths of non-geometrically similar specimens*

Boundary effect on the concrete strength is reflected in many experimental observations available in the literature (e.g. Higgins & Bailey 1976, Shinohara et al. 1991). Shown in Figure 4 are the experimental results measured on a concrete with the maximum aggregate size of 20 mm and water/cement ratio of 0.55 (Shinohara et al. 1991). The experiments were designed to test the influence of the notch depth on the concrete strength and were performed using 3PB specimens of 100×100×400 mm^3 with span of 300 mm. Two sets of concrete beams, which aged 28 days and 1 year, respectively, were loaded with a fixed cross head speed of 0.005 mm/min.

The nominal strength σ_n and equivalent crack a_e are calculated using the sizes and peak loads reported in the original paper. The nominal strength σ_n is plotted against crack length a in Figure 4a, and shows the trend that is similar to that in Figure 2b.

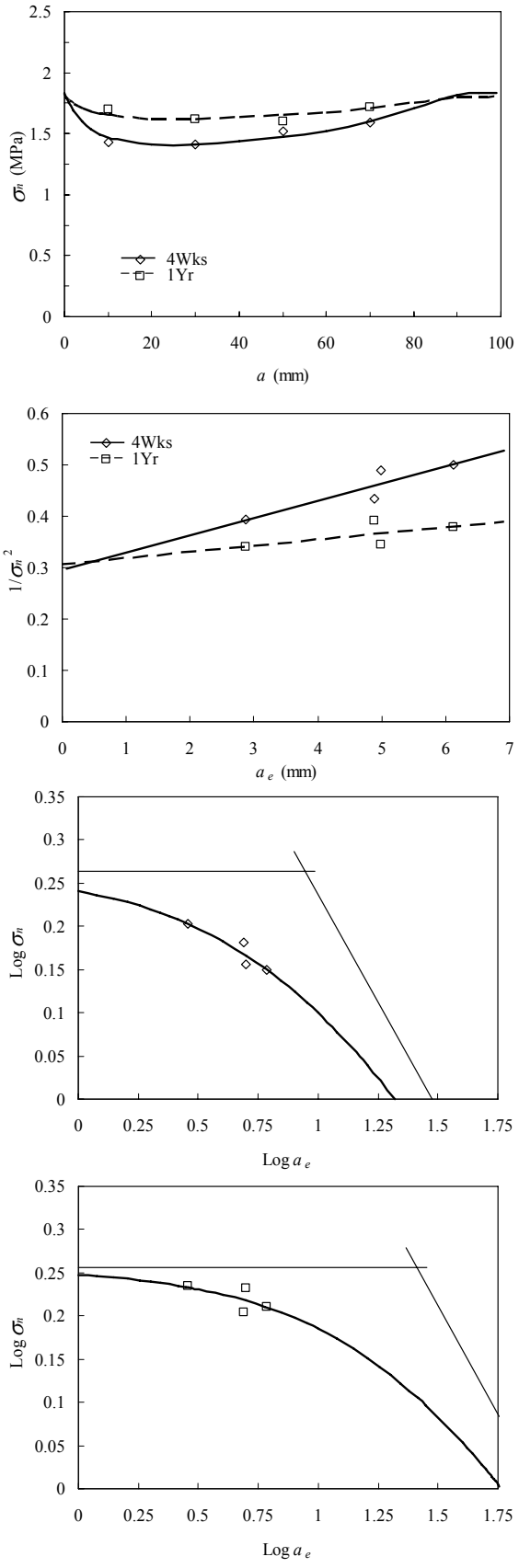

Figure 4. Boundary effects on σ_n of a concrete measured using 3PB (Shinohara et al. 1991): (a) σ_n variations with α-ratio; (b) the linear relationship between $1/\sigma_n^2$ and a_e; and (c) the comparison of 3PB σ_n with the large plate and the two asymptotes, σ_n and K_{IC} criteria.

The experimental data shown in Figure 4a can be predicted using the asymptotic boundary effect model. For this purpose, the linear form of the results given in Figure 4a is re-plotted in Figure 4b. Applying Equation 11 to these data, the material strength f_t and reference crack a^*_∞ are calculated as 1.84 MPa and 8.84 mm for 28 day concrete, and 1.80 MPa and 25.84 mm for 1 year concrete, respectively. Substituting f_t and a^*_∞ values into Equation 2, the fracture toughness is obtained as 0.34 and 0.58 MPa·√m for 28 day concrete and 1 year concrete, respectively. The solid curves shown in Figure 4a are the predictions using the above parameters and Equation 10, and show good agreement. Furthermore, the predicted and measured strength data are plotted in the system of Log σ_n versus Log a_e in Figures 4c and 4d to compare with the two asymptotic failure criteria, and show consistency with the boundary effect concept.

4.2 *Strengths of geometrically similar specimens*

Since the paper, "Size effect in blunt fracture: concrete, rock, metal" by Bažant was published in 1984, considerable research efforts have been made to explore both experimentally and theoretically the strength behaviours of geometrically similar specimens. Many experiments have been performed and documented in the literature (Bažant 1984, 1999, Carpinteri et al 1995, Karihaloo 1999, Karihaloo et al. 2003). Among these studies, Karihaloo and colleagues reported a systematic study on the "size effect" in the strength of a few concrete materials (Karihaloo et al. 2003). Shown in Figure 5 are the strength behaviours of a high strength concrete (HSC) measured on geometrically similar specimens (Karihaloo et al. 2003). The experiments were carried out using three sets of 3PB specimens with a fixed span-to-depth ratio of 4 and α-ratios of 0.05, 0.1 and 0.3.

To follow most "size effect" studies, the "gross" area based nominal strength σ_N is plotted against specimen size W in Figure 5a where it is seen that for each α, a curve of Log σ_N versus Log W can be drawn. To use the SEL to predict the strength of the three sets of geometrically similar specimens, Equation 12 has to be applied to every data set. Only the parameters A_1 and W_1 obtained from the specimens with same α value can be used to predict the strength of these specimens. Therefore, the predictions based on the different α values cannot be done.

On other hand, the predictions based on the different α values can easily be made using the boundary effect model because the parameters given in Equation 10 or 13 relate explicitly to the specimen geometry. For example, the strength data of α = 0.1 in Figure 5a can be used to calculate the parameters needed for the prediction. For this purpose, the linear form of the 3PB specimens with α = 0.1 is displayed in Figure 5b. From the linear plot, the fracture parameters f_t, a^*_∞ and K_{IC} are estimated as 11.20 MPa, 5.56 mm and 1.66 MPa√mm, respectively. Substituting the parameters back into Equation 13, the nominal strength σ_N of the specimens with α = 0.05 and 0.3 is predicted, and is plotted in Figure 5a to compare with the measured strength. It can be seen that the excellent agreements are achieved.

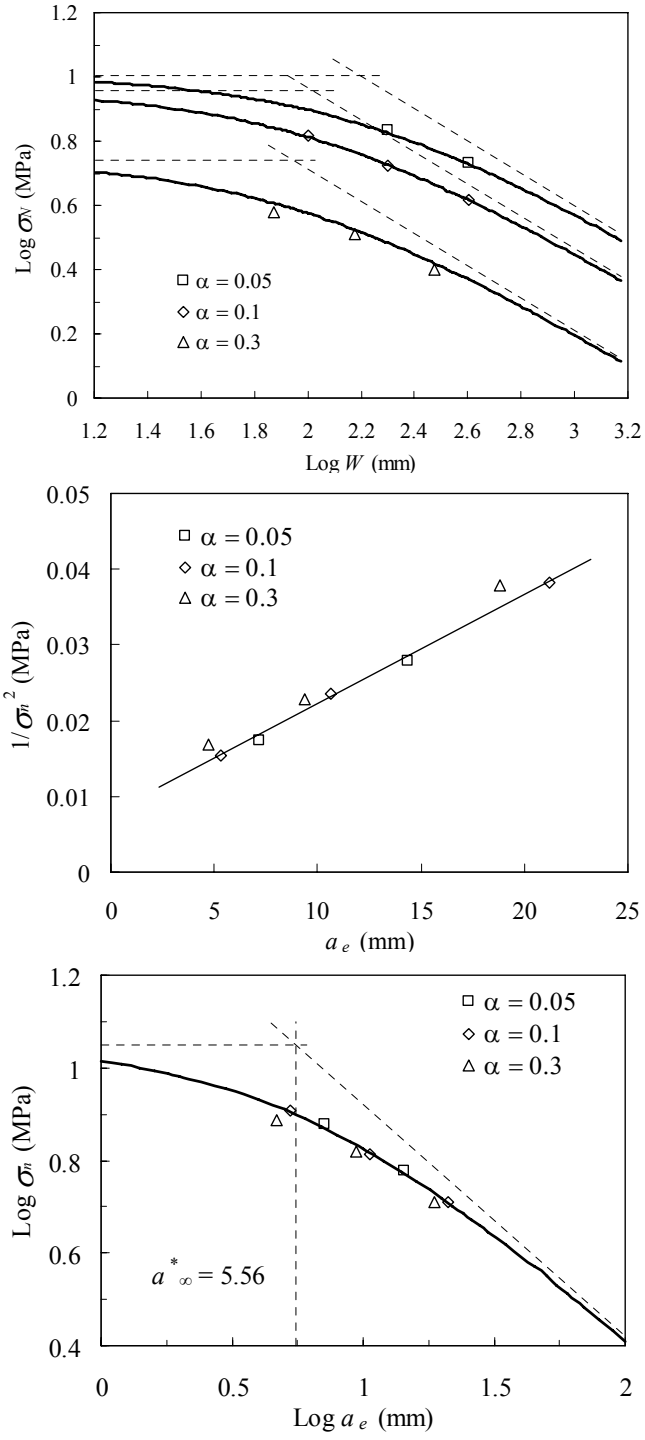

Figure 5. (a) The comparison of σ_n of a HSC (Karihaloo et al, 2003) measured on geometrically similar 3PB specimens with those predicted using Equation 10; (b) the $1/\sigma_n^2$-a_e plots for 3PB specimens with α = 0.1 used for estimating the parameters in Equation 10; and (c) the comparison of the asymptotic curve with those measured showing the unique relationship for all three α-ratios.

When the results in Figure 5a are plotted in the system of Log σ_n versus Log a_e (Fig. 5c), all the measured results follow the same curve. This is why the predictions based on different α values can be made.

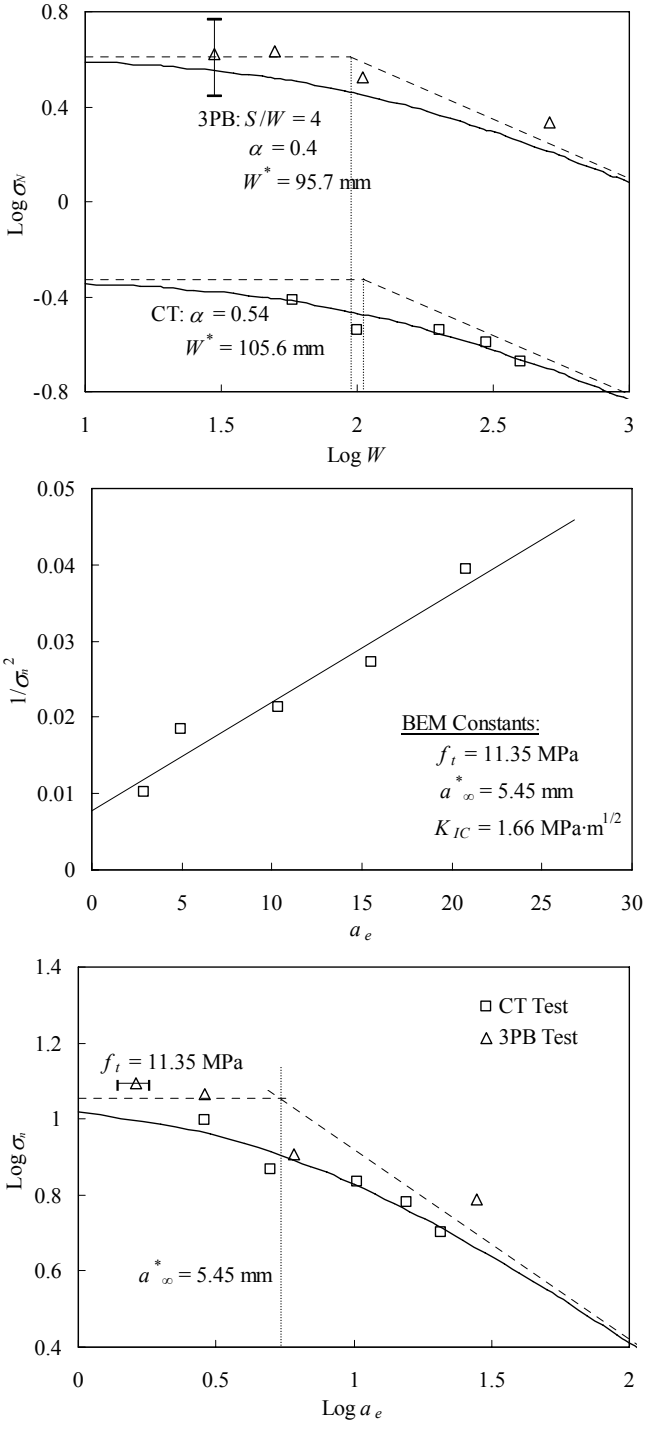

Figure 6. (a) The comparison of σ_n of a granite from a quarry in Iidate, Fukushima prefecture, Japan (Hashida & Takahashi 1985) measured on CT and 3PB specimens with those predicted using Equation 10; (b) the $1/\sigma_n^2$-a_e plots for CT specimens used for estimating the parameters in Equation 10; and (c) the comparison of the asymptotic curve with those measured showing the unique relationship for both CT and 3PB specimens.

4.3 *Strengths of different specimen geometries*

It is common that the fracture behaviour is measured using different geometries because of the availability of materials. An example is shown in Figure 6 where the fracture behaviours of a granite from a quarry in Iidate, Fukushima prefecture, Japan are tested using both compact tensile (CT) and 3-point-bend specimens (Hashida & Takahashi 1985). As shown in Figure 6a, the strength values measured on both specimen geometries show evident size dependence.

The original data show that the specimens used for the experiments are not exactly geometrically similar because α ratios for both CT and 3PB specimens are not constants. To apply the SEL to the experimental results, the α ratios for both the CT and 3PB specimens are averaged, and then, Equation 12 is used to curve-fit the CT and 3PB data to estimated the empirical parameters for the two specimen geometries (Bažant & Kazemi 1990).

In a contrast, the averaging calculation of the α-ratios for either CT or 3PB specimens is not needed when using the asymptotic boundary effect model. For an α value, the $1/\sigma_n^2$-a_e plots will follow the same linear relationship. Furthermore, only the data from one geometry are needed to calculate two of the three fracture parameters, f_t, a^*_∞ and K_{IC}.

To demonstrate, in the present study, the flexibility and effectiveness of the asymptotic boundary effect model, the strength results measured on CT specimens will be used to predict the strength of both 3PB and CT specimens. For this purpose, the σ_n values measured on CT specimens are plotted in the linear form of $1/\sigma_n^2$ versus a_e in Figure 6b. Applying Equation 11 to the plots in Figure 6b, the fracture parameters f_t, a^*_∞ and K_{IC} are obtained as 11.35 MPa, 5.45 mm and 1.66 MPa$\sqrt{}$mm, respectively. The predictions using these parameters and Equation 10 are plotted in Figure 6a to compare with those measured on both 3PB and CT specimens. It is clearly seen that the predictions agree well with those results measured on both geometries. Furthermore, Figure 6c shows all the measurements and predictions in the system of Log σ_n versus Log a^*_∞, and it can be found that these data follow the same curve as predicted by the asymptotic boundary effect model.

5 CONCLUSION REMARKS

The boundary effect concept and associated asymptotic model discussed in this paper are based on the two classical strength theories, the maximum tensile stress theory and LEFM criterion, and reflect the role of specimen boundaries in dominating the failure mode and therefore, strength of fracture specimens. The fracture behaviours predicted using the model are consistent with those observed in the frac-

ture tests of many engineering materials, i.e. specimens with short crack or ligament will fail in a "ductile" manner while the failure of those with crack tip that is far away from either boundary is dominated by the LEFM.

The important distance of the crack tip to either the front and/or back boundary is measured by the equivalent crack length a_e. By introducing the new parameter a_e, the strength behaviours of finite-sized specimens are made equivalent to the simple case of the large plate where only the front boundary influences specimen fracture. As a result, the strength data measured on all types of fracture mechanics specimens – non-geometrically similar specimens, geometrically similar specimens with different α ratios and different testing geometries – will follow the same relationship in the system of (Log) σ_n versus (Log) a_e. This is important because it establishes the basis for predicting the strength behaviours from the data measured on the specimens of different geometries.

It is demonstrated that the "size effect" in the fracture of geometrically similar specimens is a special case of the boundary effect. The SEL, Equation 12 can be derived from the boundary effect model by setting a constant α as shown in Equation 13b. However, it is more important that the asymptotic boundary effect function for geometrically similar specimens, Equation 13b gives explicit expressions for the two parameters that have to be measured on the specimens with the same geometry when using the SEL. Therefore, the asymptotic equation 13b can be used to predict the strength behaviours of a set of geometrically similar specimens using the data obtained from other sources.

Analysis of the literature data shows that both fracture toughness K_{IC} and strength f_t can be calculated from the strength measurements. This is different from the SEL where the tensile strength f_t has to be measured in a separate test.

ACKNOWLEDGEMENT

The financial support from the Australian Research Council (ARC) under the scheme of Discovery Grant is acknowledged.

REFERENCES

Bažant, Z.P. 1984. Size effect in blunt fracture: concrete, rock, metal. *J Eng Mech (ASCE)* 110(4): 518-35.

Bažant, Z.P. 1999. Size effect on strength: a review. *Arch Appl Mech* 69: 703-25.

Bažant, Z.P. & Kazemi, M.T. 1990. Determination of fracture energy, process zone length and brittleness number from size effect, with application to rock and concrete. *Int J Fract* 44: 111-131.

Carpinteri, A., Chiaia, B. & Ferro G. 1995. Size effects of nominal tensile strength of concrete structures: multifractality of material ligaments and dimensional transition from order to disorder. *Mater Struct* 28: 311-17.

Duan, K. & Hu, X.Z. 2002. Asymptotic analysis of boundary effects on fracture properties of notched bending specimens of concrete. In A.V. Dyskin, X.Z.. Hu & E. Sahouryeh (eds), *Structural Integrity and Fracture (Proc SIF 2002)*: 19-24. Lisse, Netherlands: A.A.Balkema Publishers.

Duan, K. & Hu, X.Z. 2004. Specimen boundary induced size effect on quasi-brittle fracture. *Strength, Fracture and Complexity* 2 (2): 47-68.

Duan, K., Hu, X.Z. & Wittmann F.H. 2002. Explanation of size effect in concrete fracture using non-uniform energy distribution. *Mater Struct* 35: 326-31.

Duan, K., Hu, X.Z. & Wittmann F.H. 2003a. Thickness effect on fracture energy of cementitious materials. *Cem Concr Res* 33 (4): 499-507.

Duan, K., Hu, X.Z. & Wittmann F.H. 2003b. Boundary effect on concrete fracture and non-constant fracture energy distribution. *Eng Fract Mech* 70: 2257-68.

Duan, K., Hu, X.Z. & Wittmann F.H. 2004. Boundary effects and fracture of concrete. In V.C. Li, C.K.Y. Leung, K.J. Willam, & S.L. Billington (eds), *Fracture Mechanics of Concrete Structures (Proc. FraMCoS-5)*: 205-212. Ia-FraMCoS.

Duan, K., Hu, X.Z. & Wittmann F.H. 2006. Asymptotic analysis of boundary effects on fracture properties of quasi-brittle materials. *Mech Mater* 38: 128-141.

Hashida, T. & Takahashi, H. 1985. Simple determination of the effective young's modulus of rock by the compliance method. *J Testing Evaluation* 13: 77-84.

Higgins, D.D. & Bailey J.E. 1976. Fracture measurements on cement paste. *J Mater Sci* 11: 1995-2003.

Hillerborg, A., Modeer, M. & Petersson, P.E. 1976. Analysis of crack formation and crack growth in concrete by means of fracture mechanics and finite elements. *Cem Concr Res* 6: 773-82.

Hu, X.Z. & Duan, K. 2002. Size effect and crack bridging in coarse-microstructure composites. In A.V. Dyskin, X.Z.. Hu & E. Sahouryeh (eds), *Structural Integrity and Fracture (Proc SIF 2002)*: 43-48. Lisse, Netherlands: A.A.Balkema Publishers.

Hu, X.Z. & Wittmann, F.H. 2000. Size effect on toughness induced by crack close to free surface. *Eng Fract Mech* 65: 209-21.

Jenq, Y. & Shah, S.P. 1985. Two parameter fracture model for concrete. *J Eng Mech (ASCE)* 111 (10): 1227-1241.

Kaplan, M.F. 1961. Crack propagation and the fracture of concrete. *ACI Journal* 58: 591-610.

Karihaloo, B.L. 1999. Size effect in shallow and deep notched quasi-brittle structures. *Int. J. Fract*. 95: 379-390.

Karihaloo, B.L., Abdalla, H.M. & Xiao, Q.Z. 2003. Size effect in concrete beams. *Eng Fract Mech* 70: 979-993.

Nallathambi, P., Karihaloo, B.L. & Heaton, B.S. 1985. Various size effects in fracture of concrete. *Cem Concr Res* 15: 117-26.

Shinohara, Y., Furumura, F. & Abe, T. 1991. Softening behaviour of concrete in three-point bend test on single edge notched beams. In J.G.M. Van Mier, J.G. Rots & A. Bakker (eds), *Fracture processes in concrete, rock and ceramics*: 523-32. London: E & FN Spon.

Tada, H., Paris, P.C. & Irwin, G.R. 2000. *Stress Analysis of Cracks Handbook, 3rd Ed*. New York: ASME Press.